Available online www.jsaer.com

***Journal of Scientific and Engineering Research*, 2019, 6(4):188-193**

Research Article

ISSN: 2394-2630
CODEN(USA): JSERBR

Theoretical study of a near-field thermophotovoltaic photocell based on SiC and InGaAsSb

Waly DIALLO*, Saliou NDIAYE, Mamadou NIANE, Omar. A. NIASSE, Bassirou BA

Laboratoire de semi-conducteurs et d'énergie solaire, Département de physique, Faculté des sciences et techniques (UCAD-SENEGAL).
walydiallo85@yahoo.fr

Abstract Near-field thermophotovoltaic conversion offers real prospects. The contribution of evanescent waves is very significant at small scales. The work we have done has theoretically proved it. Whether it's the flux, the electrical power and the energy conversion efficiency, all of its parameters have proved it. The SiC-InGaAsSb tandem is an excellent transmitter-absorber pair operating in the near field. The efficiency can exceed 80% contrary to the 33%. However, this efficiency does not take into account optical and parasitic factors.

Keywords Near-field, thermopotovoltaic, SiC, InGaAsSb, efficiency

Introduction

The efficiency limit of a thermo-photovoltaic (TPV) system is related to the emissivity of the emitter on the spectral plane. This is true for systems operating in the far field TPV system, where the distance between the emitter and the photovoltaic cell is large enough to limit energy transfer only to modes propagating in the air. In contrast, in the near field, when the distance between the two surfaces is smaller than that of the wavelength, the limit is raised. It has been theoretically argued and demonstrated experimentally that the separation distance can greatly improve the energy transfer with respect to the far field and even the black body [1, 2]. In the case of the near field, thermal radiation can be defined as electromagnetic waves emitted due to the random fluctuation of charges in the material [3,4].

Silicon carbide

Silicon carbide is an excellent emitter because of its interesting thermal properties which are in line with absorbers such as low gap semiconductor materials including InGaAsSb. Silicon carbide can adapt to high temperatures, radiative environments, high pressure, high field due to its wide bandgap refractory semiconductor structure. That is why we chose it to form with InGaAsSb a emitter-cell tandem pair in a TPV cell. The emission spectrum of the silicon carbide is adequate to the absorption spectrum of the cell. SiC is subject to polymorphism which results in the existence of many polytypes. Polytypes have the same structure and chemical composition, but the stacking of the crystallographic base unit differs [5,6].

Theoretical study on a far-field TPV device based on InGaAsSb

Nowadays TPV prototypes are available after lengthy research, even if there are many things to accomplish to achieve the best efficiency. Their fields of application are numerous, which is why his research arouses a great deal of interest. These prototypes are often based on GaSb or InGaAs. Their banned bands are between 0.3ev and 0.7eV. Their emission temperature is between 1200 °C and 1700 °C. They are not expensive and are environmentally friendly [6,7]. A efficiency of 19% is obtained for these cells with a band gap of $In_xGa_{1-x}A_ySb_{1-y}$ of 0.53 eV, a power density of 0.58 W, a radiation temperature of 950 °C and that of the 27 °C diode [7]. Its

role is to convert the heat from the emitter into electricity. It consists of a junction of two doped semiconductors p and n. The conversion of incident photons into electricity is possible only if their energy is greater than that of the forbidden band of the semiconductor. The low energy photons are then lost in the cell in the form of heat, which is detrimental to the durability of the cell.

The PN junction results from the juxtaposition of two zones in the same semiconductor material; one of type P (majority in holes, minority in electrons) and the other of type N (majority in electrons, minority in holes).

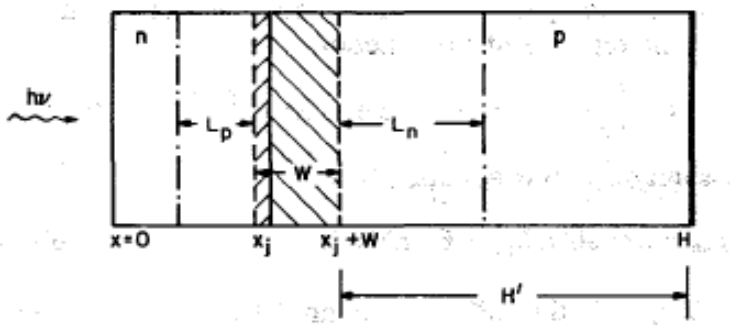

Figure 1: Polarization of the PN junction [8]

Results and Discussion

Near-field radiative heat flux

In heat transfer analyzes, we are mainly interested in the radiation heat flux given by the mean time of the Poynting vector [9]:

$$\langle S(x,\omega)\rangle = 4\ X\ \frac{1}{2} Re\langle E(x,\omega)\ X\ H*(x,\omega)\rangle \quad (1)$$

This expression of the Poynting vector gives a value four times larger than its usual definition, since only the positive frequencies are considered in the Fourier decomposition of the efficiency. The substitution of the expression of the electric and magnetic fields defined previously gives us, [9]:

$$\langle S(r,\omega)\rangle = 2\omega\mu_V\ \mathcal{R}e[i\int_{V'} dV' \int_V dV\ G^{E}_{;m\alpha}(r, r', \omega)\ G^{H*}_{;n\beta}(r, r'', \omega')\ \langle J^{r}_{\alpha};(r', \omega)\ J^{r*}_{\beta};(r'', \omega')\rangle] \quad (2)$$

The indices m and n represent the state of polarization of the fields observed in r, then αrepresents the state of polarization of the source in r. The set of indices mα implies that a summation is performed on all the components (ie xx + xy + ... + zz). At this point, the radiant heat flux can be calculated from:

$$\langle S(r,\omega)\rangle = \frac{2k_V^2\Theta(\omega,T)}{\pi} Re[i\varepsilon'_r(\omega)\int_{V'} dV'\ G^{E}_{m\alpha}(r,r',\omega)G^{H*}_{n\beta}(r,r'',\omega')] \quad (3)$$

where k_v is the amplitude of the wave vector in vacuum.

After simplification [9, 10]: there is an upper limit of radiative heat flux in the near field, for non-magnetic materials, this is given by:

$$q''_{max} = X_{max}\frac{K_B^2}{6\hbar}(T_1^2 - T_2^2) = \frac{K_B^2\beta_c^2}{48\hbar}(T_1^2 - T_2^2) \quad (4)$$

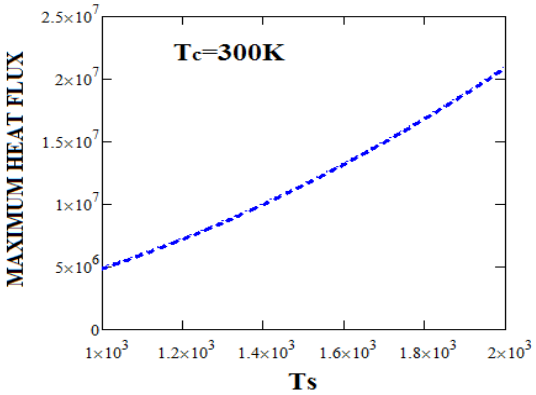

Figure 2: Maximum flow depending on the emitter temperature

q "max is the maximum heat flux, it is obtained when d → 0. It is found that metals with a large imaginary part in the infrared can help to reach such a limit at extremely small distances. However, for distances greater than a few nanometres, the situation is different.

Heat flows according to the distance

The dependence in 1 / d2 of the heat flux concerns the contribution through the polarization p of the electromagnetic waves only, since the contribution through the polarization s will be reached asymptotically to a constant close since d → ∞ [11].

Equation (10) becomes:

$$\phi_0(Ts,d)=\frac{\hbar\omega_0^2}{4\sigma k T_e^5}\frac{e^{\frac{\hbar\omega_0}{kTe}}}{\left[e^{\frac{\hbar\omega_0}{kTe}}-1\right]^2}\cdot\frac{\chi}{4\pi d^2} \quad (5)$$

$u=\frac{\hbar\omega_0}{kTe}$ which is a normalizing quantity then is a constant that strongly depends on the optical characteristics of the emitting material. Our calculations give a maximum value of $6.47.10^{-18}$ of.

$$\phi_0(Ts,d)=\frac{\chi\omega_0}{16\pi\sigma Te^4 d^2}\frac{u.e^u}{\left(e^u-1\right)^2} \quad (6)$$

Or $W_0=\sqrt{\frac{e_\infty W_L^2+W_T^2}{e_\infty+1}}$

For the silicon carbide that we considered here as our emitter, we have: $\varepsilon_\infty = 6.7$; $\omega_L = 18.253\ 10^{13}$ rad.s^{-1}; $\omega_T = 14.937\ 10^{13}$ rad^1.s Γ =89.66 10^{10} rad.s^{-1}

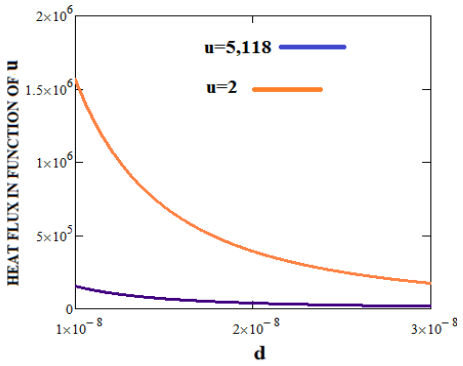

Figure 3: heat flow according to u and distance

By maintaining the value of u = 2, we have drawn on the figure the ideal heat flux as a function of the distance d. This distance is of the order of one nanometre. The figure shows a clear dependence of the flow compared the distance d. This dependence is almost exponential.

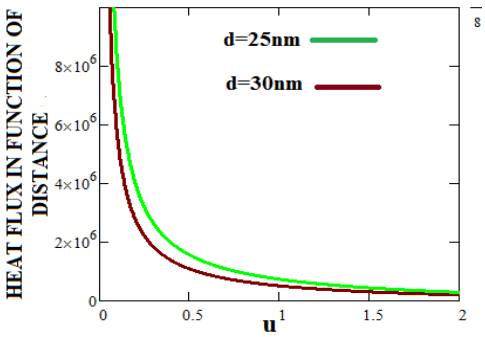

Figure 4: heat flux as a function of temperature and distance

As for the figure, we have on the abscissa axis, u and on the ordinate axis, the heat flux which is also a function of the distance. Once again the phenomenon observed in the previous figure resurfaced. That is, the dependence of flux on small distances.

In reality, when the InGaAsSb-based cell is placed near the silicon carbide (SiC) emitter, the evanescent waves of SiC reinforce the ever-existing progressive waves whatever the distance. When the SiC moves away from the InGaAsSb, the evanescent waves disappear and no longer contribute to the flow exchange.

Electric power

The power generated in the photodiode is calculated as the product of the voltage V_0, e the charge of the electron, and the difference between the absorbed photon flux and the re-emitted photon flux [12]:

$$P_{PV} = \frac{1}{\pi^2}\int_0^{\infty} dqq\left[\int_{\omega_g}^{\infty} d\omega\Pi(\omega,q)\frac{eV}{e^{\left(\frac{\hbar\omega}{kTe}\right)}-1} - \int_{\omega_g}^{\infty} d\omega\Pi(\omega,q)\frac{eV_0}{e^{\frac{\hbar\omega-eV_0}{kT_S}}-1}\right] \tag{7}$$

$$\Pi(\omega,q) = \frac{\mathrm{Im}\left(\frac{\varepsilon_1-1}{\varepsilon_1+1}\right)\mathrm{Im}\left(\frac{\varepsilon_2-1}{\varepsilon 2+1}\right)}{\left|1-\left(\frac{\varepsilon_1-1}{\varepsilon_1+1}\right)\left(\frac{\varepsilon_2-1}{\varepsilon_2+1}\right)e^{-2qd}\right|^2}e^{-2qd} \tag{8}$$

V_0 is the potential difference at which the cell operates, q is a component of the wave vector; ε_1 and ε_2 are the dielectric functions of the emitter and the cell respectively; d is the distance between the source and the cell; ω_g is the frequency of the gap of the cell.

$$V_0^{\max} = \omega_g\left(1-\frac{T_S}{T_e}\right) \tag{9}$$

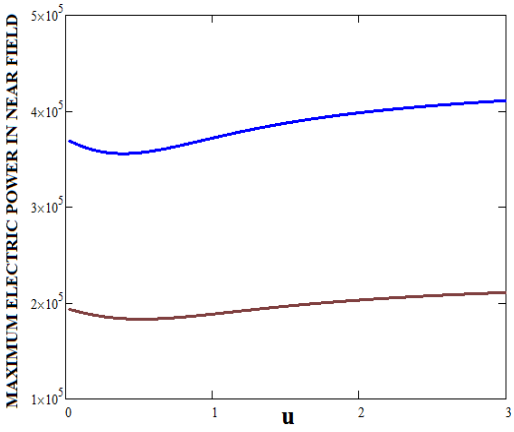

Figure 5: dependence of the maximum electric power in the near field as a function of u

The ordinate shows the maximum electrical power in the near field and the normalization quantity u in the abscissa. this power is very important especially compared the corresponding power in far field. However this power also varies according to u. the large values of u (greater than 6) go out of the infrared range and end up in the visible wavelength range.

Expression of performance

$$\eta = \frac{P_{El}}{P_{rad}} \tag{10}$$

Its expression according to the near-field distance is as follows:

$$\eta = \frac{\int_0^\infty dqq\left[\int_{\omega_g}^\infty d\omega\Pi(\omega,q)\frac{eV}{e^{\left(\frac{\hbar\omega}{kTe}\right)}-1} - \int_{\omega_g}^\infty d\omega\Pi(\omega,q)\frac{eV_0}{e^{\frac{\hbar\omega-eV_0}{kT_S}}-1}\right]}{\int_0^\infty dqq\left[\int_0^\infty d\omega\Pi(\omega,q)\frac{\hbar\omega}{e^{\left(\frac{\hbar\omega}{kT_e}\right)}-1} - \int_{\omega_g}^\infty d\omega\Pi(\omega,q)\frac{\hbar\omega}{e^{\frac{\hbar\omega-eV_0}{kT_S}}-1}\right]} \quad (11)$$

We are dealing here with the upper limit of the efficiency for near field thermal radiation, which is similar to near-monochromatic radiation treated by thermodynamics [13, 14]. This radiation is largely dominated by the frequency of the resonance mode. That is why this efficiency corresponds to that of a quasi-monochromatic source [13]. We observe the increase in near-field efficiency as the resonant frequency increases but also as the temperature increases. Which corresponds to that of a near-monochromatic radiation.

$$\eta_{LIM} = 1 - \frac{\chi(\omega)-1}{\chi(\omega)-1} + \frac{k_B T_e}{\hbar\omega_0}(\chi(\omega)-1)\left\{\begin{array}{l}\left[1+\frac{1}{\chi(\omega)-1}\right] \\ \ln\left[1+\frac{1}{\chi(\omega)-1}\right]+\left(\frac{1}{\chi(\omega)-1}\right)\ln(\chi(\omega)-1)-\left[1+\frac{1}{\chi(\omega)-1}\right] \\ \ln\left[1+\frac{1}{\chi(\omega)-1}\right]+\left(\frac{1}{\chi(\omega)-1}\right)\ln(\chi(\omega)-1)\end{array}\right\} \quad (12)$$

$$n(w,T) = \frac{1}{c(w)-1}$$

and

$$c(w) = \exp\left(\frac{hw_0}{K_B T_{Ce}}\right)$$

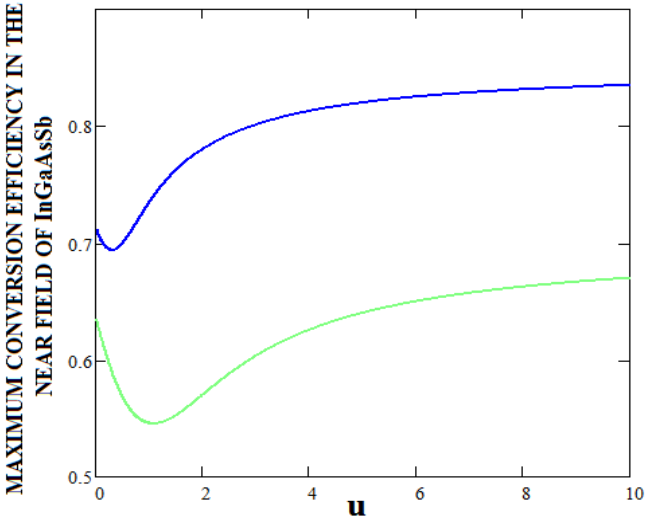

Figure 6: dependence of the maximum conversion efficiency as a function of u

Efficiencies can reach 80% above those predicted by thermodynamics (33%). This surplus efficiency can't be explained by the contribution of evanescent waves.

Conclusion

Silicon carbide and InGaAsSb are important tandems for near-field thermophotovoltaic conversion. Like any emitter, SiC has surface waves that are confined to the surface and disappear at nanometric distances.

Whether it's the flow, the maximum electrical power extracted and the TPV conversion efficiency, the tandem offers real hopes for a good conversion of heat into electricity. The problem to be solved is the adaptation of silicon carbide to high temperatures. For this, we can think of incorporating a cooling system.

Reference

[1]. S. H. Brewer and S. Franzen, *Calculation of the electronic and optical properties of indium tin oxide by density functional theory*, Chem. Phys. 300, 285–293, 2004.

[2]. C. H. Park, H. A. Haus, and M. S. Weinberg, *Proximity-enhanced thermal radiation*, J. Phy. Appl. Phys. 35, 2857–2863, 2002.

[3]. C. L. Tien, A. Majumdar and F. M. Gerner, *Microscale Energy Transport*, Washington, D.C.: Taylor & Francis, 1998.

[4]. P. Keunhanet Z. Zhang, *Fundamentals and applications of near-field radiative energy transfer*, Global Digital Central, vol. 4, 11.3001, 2013.

[5]. Adrien DENEUVE, *synthese et caracterisations de supports de catalyseurs nano-macro à base de carbure de silicium. Application à l'oxydation catalytique du sulfure d'hydrogene en soufre elementaire,* These de doctorat, UNIVERSITE DE STRASBOURG, 2010

[6]. B.J. Nel, S. Perinpanayagam, A brief overview of SiC MOSFET failure modes and design reliability, The 5th International Conference on Through-life Engineering Services , ELSEVIER 2017

[7]. Michael W. Dashiell et al, *quaternary InGaAsSb thermophotovoltaic diodes*, IEEE; Volume: 53 ,12 ;2006

[8]. MacMurray D. Whale and Ernest G. Cravalho, *Modeling and performance of microscale thermophotovoltaic energy conversion devices*, IEEE; Volume: 17; p. 130 - 142; 200.

[9]. Berkaï Zakaria, *Etude et simulation d'une cellule thermo-photovoltaïque,* mémoire, UNIVERSITE DE BECHAR Faculté des Sciences et Technologie, 2012

[10]. C. T. Andrew, *The thermal near-field: Coherence, spectroscopy, heat-transfer, and optical forces, Elsevier*, vol. 88, 2013.

[11]. J. Karl, *Transferts aux petites échelles: application au rayonnement thermique, aux forces de Chermiqueasmir et à la conduction*, Poitiers: Université de Poitiers, 2006.

[12]. L. Ivan, P.-M. Agustin et M. R. J., *Thermodynamics and energy conversion of near-field thermal radiation: Maximum work efficiency bounds*, EDP Sciences, vol. 79,101001, 2014.

[13]. P. Keunhanet Z. Zhang, *Fundamentals and applications of near-field radiative energy transfer*, Global Digital Central, vol. 4, 11.3001, 2013.

[14]. L. Ivan, P.-M. Agustin and M. R. J., *Thermodynamics and energy conversion of near-field thermal radiation: Maximum work efficiency bounds*, EDP Sciences, vol. 79, 101001, 2014..

[15]. N. Arvind et Z. Yi, *Theory of thermal nonequilibrium entropy in near-field thermal radiation*, PHYSICAL REWIEW, vol. 88, 1075412; 2014